Polar Geosci , **15**, 123-147, 2002

Hydrostatic investigations on subglacial meltwater: implications for the formation of streamlined bedforms and subglacial lakes, East Antarctica

Takanobu Sawagaki and Kazuomi Hirakawa

Graduate School of Environmental Earth Science, Hokkaido University, Sapporo 060-0810

Abstract: Streamlined bedforms and small erosional marks observed on the Sôya Coast, East Antarctica, are interpreted to have been formed by subglacial meltwater The source of water is attributed to subglacial lakes that may have existed beneath the upper part of the Mizuho Plateau In order to evaluate the subglacial meltwater hypothesis, two theoretical investigations were carried out, one to model the formation of subglacial lakes in the Shirase drainage basin, and the second to estimate the conformity of water flow beneath the ice sheet to underlying topography In the first investigation we found that several subglacial lakes would have formed in the bed depressions with the water surfaces determined by englacial equipotential surfaces In the second investigation, several ice thicknesses and their surface gradients were determined in which agreement between potential gradients and the observed bedform distribution was found These experimental results add to the existing observations and inductive reasoning supporting a subglacial hydraulic origin for bedforms along the Sôya Coast According to the results, possible causes of sudden subglacial outburst floods and their influence are discussed If subglacial water storage and sudden discharge occurred, a combination of water accumulation beneath the ice sheet and discharge of this water could make the ice sheet unstable leading to the rapid melting of the ice sheet supplying huge amount of meltwater to the ocean and formation of local ice streams Such subglacial meltwater events in Antarctica possibly contributed some global meltwater pulse events during MIS-3 or post-LGM periods

key words streamlined bedform, subglacial lake, meltwater, East Antarctica

1. Introduction

During the last two decades, there has been much debate regarding subglacial landforms and their formative processes drumlins formation has been a central part of this discussion (*e g* Menzies and Rose, 1989, Dardis and McCabe, 1994, Sawagaki and Hirakawa, 1998) Traditionally, drumlin-like forms were thought to have been the product of normal processes of subglacial erosion and sediment deposition (*e.g* Boulton, 1974, 1979) A semi-quantitative flow model for the rapid subglacial deformation of soft sediments and the formation of drumlins was also developed on the basis of field observations and measurements (*e.g.* Boulton, 1979, Boulton and Hindmarsh, 1987)

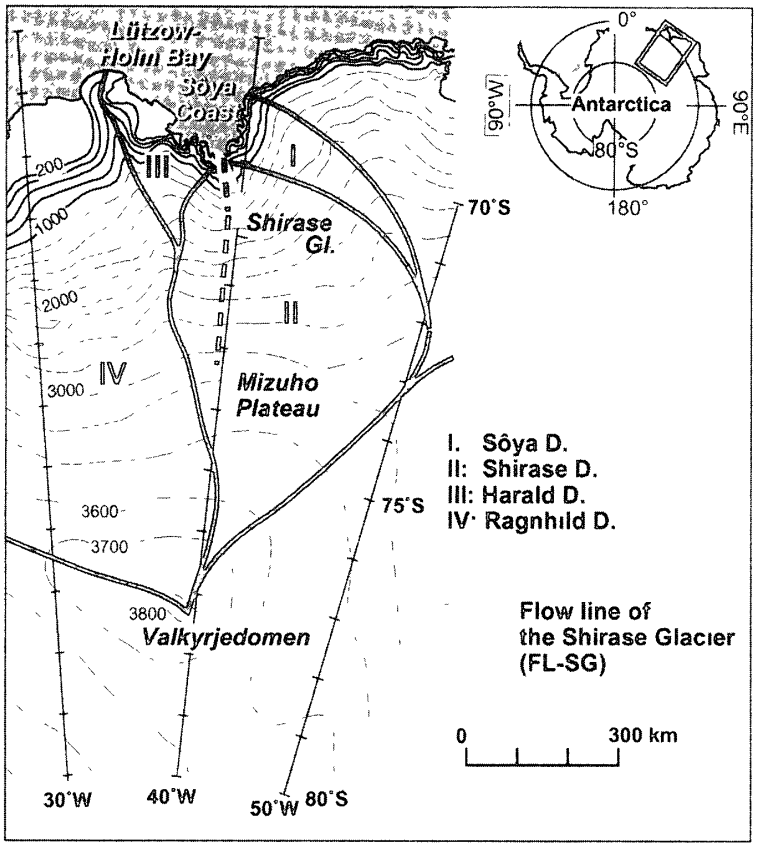

Fig 1 Surface topography and subdivisional drainage basin of the Antarctic Ice Sheet in Mizuho Plateau, East Antarctica (modified from the ice sheet surface map in National Institute of Polar Research, 1997)

Recently Hindmarsh (1998a, b) explained drumlin formation by viscous till mechanisms However, these studies focused mainly on subglacial sediment deformation and are not applicable to glacial landforms in hard bedrock By contrast, Shaw and his co-workers have advocated that subglacial streamlined erosional bedforms were formed by turbulent subglacial meltwater (*e g* Shaw, 1996, 2002 and refs therein) In theoretical studies, Shoemaker (1991, 1992a, b) considered that the source of large floods emerging from the Laurentide Ice Sheet was a mega-subglacial lake in the Hudson Bay basin

Along the Sôya Coast, East Antarctica, Sawagaki and Hirakawa (1997) described subglacial streamlined bedforms and accompanying small erosional marks, and suggested that these forms represent past meltwater floods beneath the Antarctic Ice Sheet They speculated that the reservoir had been subglacial lakes beneath the upper reaches of the Shirase Glacier, Mizuho Plateau (Fig 1) Although a number of subglacial lakes are known to exist beneath the present Antarctic Ice Sheet (*e g* Siegert, 2000 and refs therein), the following uncertainties challenge the speculation 1) according to the inventory of Antarctic sub-glacial lakes (Siegert *et al*, 1996), no subglacial lakes are mapped on the Mizuho Plateau, 2) water storage or subglacial drainage seems unlikely in the coastal zone beneath the Antarctic Ice Sheet where the thin ice may have been cold-based, and 3) it is highly improbable that discharges associated with steady state pressure melting can produce the volume of water required to form large channels (Sugden *et al*, 1991)

Despite these uncertainties, it is also true that the absence of subglacial lakes in Mizuho Plateau has not been demonstrated by direct observations The following studies suggest the possible existence of subglacial lakes in this region from the past to today 1) Sugden *et al* (1991), who investigated channels in a part of the Asgard Range in Antarctica, suggested that meltwater could have been produced by sudden outbursts, reflecting periodic drainage of sub-glacial lakes beneath the thick ice or by sub-glacial drainage of surface lakes 2) Nishio *et al* (1989) have calculated that the basal temperature along the flow line of the Shirase Glacier (FL-SG) (Fig 1) is at pressure melting point between 20 km and 260 km from the coast, and that the basal ice of the upper part of the basin beyond 260 km from the coast is frozen to the bed, and 3) Mae and Naruse (1978) suggested the possibility of basal sliding beneath the ice sheet of the Shirase drainage basin 200 km inland from the coast

In order to evaluate the possible role of subglacial meltwater in the areas of the Sôya Coast and Mizuho Plateau, we carried out two theoretical examinations of meltwater storage and evacuation beneath the former, more expansive Antarctic Ice Sheet along the coastal zone One is an investigation to determine the possibility of subglacial water storage along the basal sliding zone, and to estimate the reservoir size, the other is numerical modeling to estimate former ice surface gradients concerning the conformity of water flow direction beneath ice sheet to the slope of the underlying topography According to the results, possible cause of sudden subglacial outburst floods and their influence are discussed

2. Inferred subglacial lakes along the Shirase drainage basin

2.1. Mizuho Plateau, Sôya Coast, and Shirase Glacier

Mizuho Plateau lies on the northeastern slope of the second highest dome of the Antarctic Ice Sheet (Valkyrjedomen) Ice surface ridges divide the plateau into several drainage basins (National Institute of Polar Research, 1997) (Fig 1) The Shirase Glacier, the largest ice stream in the Mizuho Plateau region, pours into the head of Lutzow-Holm Bay It drains a considerable area and exerts influence on the surface morphology of the ice sheet behind the coast with which it converges toward Mizuho Plateau (Naruse and Shimizu, 1978, Shimizu *et al*, 1978)

The ice sheet in the Sôya subdivisional drainage basin forms a divergent ice flow to the Sôya Coast which results in a sheet flow (Naruse and Shimizu, 1978, Shimizu *et al*, 1978, National Institute of Polar Research, 1997) The surface of the ice margin falls rapidly to Lützow-Holm Bay, and the regional, present-day ice sheet flows approximately perpendicular to the coast Some outlet glaciers flow into Lützow-Holm Bay between ice-free areas (Fig 2) Glacial striae on the deglaciated surface along the coast show that the former ice flow was also perpendicular to the coast (Yoshida, 1983) Yoshida (1983) concluded that the ice sheet probably extended to the outer edge of the continental shelf at its maximum, and Hayashi and Yoshida (1994) concluded that major retreat of the ice sheet from the region took place prior to 35 kyr BP However, the exact time when the erosional bedforms were created is unknown

Although no subglacial lakes have been identified in Mizuho Plateau so far (*cf.* Siegert *et al*, 1996), the possibility remains that the further investigations will discover

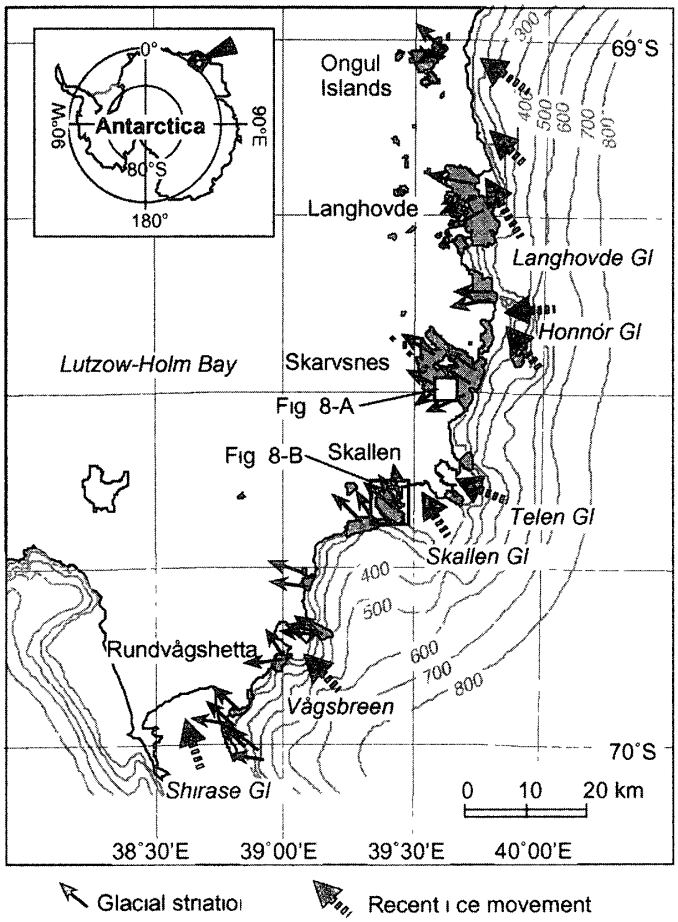

Fig 2 Index map of the Sôya Coast modified from the map of Yoshida (1983) The black arrows show former ice movement indicated by glacial striae Dashed arrows show the present ice movement

subglacial lakes in this area is still remained Subglacial meltwater would be expected to accumulate in bed depressions, and water surfaces are determined so as to be the equipotential surfaces (Shreve, 1972) According to this fundamental principle, the first investigation is performed to estimate the location and size of subglacial depressions in which subglacial water storage is likely to be ponded in Mizuho Plateau

Most of the presently ice-free areas along the Sôya Coast (Fig 2), where we are arguing erosion of bedrock by subglacial meltwater, are expected to have been influenced by the glacial activity of Sôya drainage basin (Fig 1) However, the ice thickness, ice flow direction and glacier bed topography in this drainage basin are not well known Despite this, those along FL-SG (Fig 1) are well observed compared with the other areas in Mizuho Plateau (*cf* Watanabe *et al*, 1992, National Institute of Polar Research, 1997) In addition, the calculated recent basal temperature (Nishio *et al*, 1989) and sub-ice thermal conditions inferred by radio-echo sounding (Ohmae, 1988) are also available along the same flow line Consequently, an alternative approach is to focus on FL-SG

2 2 Hydrostatic investigation

The principal theory used in this examination is that the direction of water flow in the

englacial part of the glacier hydraulic system can be expected to be normal to equipotential surfaces (Shreve, 1972) This fundamental theory is applied in the next section

Following Shreve (1972, 1985a, b), a water pressure potential surface (Φ) is defined by

$$\Phi = \Phi_O + \rho_w g z + p_w + p(\dot{r}) \tag{1}$$

where Φ_O is a reference potential, p_w is the density of water, z is the elevation of a point within or on the bed of the glacier, p_w is the pressure in the water due to the overburden pressure of ice, $\dot{r}$ is the rate of change in the radius of the water passages by plastic flow of ice and melting of ice, and $p(\dot{r})$ denotes a contribution to the pressure (or potential) that is a function of $\dot{r}$ The first term on the right is a reference potential, and the second is the potential of the water due to its height above a datum The third is the pressure in the water due to the overlying ice given by the following equation,

$$p_w = \rho_i \, g(h_I - z) \tag{2}$$

where ρ_i is the density of ice, h_I is the elevation of the ice surface The fourth term in eq (1) is a pressure difference between the water and ice that results in closure of the tunnel by plastic flow Here we assume that the gradient in $p(\dot{r})$ is small in comparison with that of the other terms, and set its value equal to zero (Hooke, 1989)

Water flows in the direction perpendicular to lines of constant Φ in eq (1) Along such lines, the gradient of Φ is zero Thus, an equipotential surface is obtained in two dimensions by differentiation of eq (1) with respect to horizontal distance x after substituting from eq (2) for p_w,

$$(\rho_w - \rho_i)\frac{dz}{dx} + \rho_i \frac{dh_I}{dx} = 0 \tag{3}$$

The relative contributions to the slope of the equipotential surfaces within a glacier (dz/dx) and the slope of the glacier surface (dh_I/dx) are given by

$$\frac{dz}{dx} = \left(\frac{-\rho_i}{\rho_w - \rho_i}\right)\frac{dh_I}{dx} \tag{4}$$

It is readily shown by this equation that the equipotential surfaces dip upglacier with a slope of about 11 times the slope of the glacier surface Thus, under the hydrostatic model basal meltwater might be accumulated in bed depressions, provided the relationship $11\alpha < \gamma$ is satisfied (Oswald and Robin, 1973, Shoemaker, 1991) Here, α is the ice-surface gradient, positive if the ice surface slopes downglacier, and γ is the bed slope, positive if the bed is ascending downglacier

To simplify the calculation of the englacial equipotential surface, the ice surface profile was reconstructed by integrating the equation of the ice-surface profile, assuming that the bed is horizontal (h_G=constant), and ice is a perfectly-plastic material with the yield stress τ_b,

$$(h_I - h_G)^2 = \frac{2\tau_b d}{\rho_i g}, \tag{5}$$

where d is the distance from the edge measured along the flow line, h_G is the elevation of the bed, and basal shear was assumed to be equal to 100 kPa at every point along the flow line, because Nishio *et al* (1989) noted that τ_b is approximately 100 kPa in the upper parts

of the Shirase Glacier

2.3 *Longitudinal profiles along the Shirase Glacier*

Figure 3 shows bedrock and ice surface elevations with englacial hydrostatic equipotential surfaces (A), basal shear stress profile (B), and the calculated temperature profile in the ice sheet (C) along FL-SG (Fig 1). As the calculation was performed only along one flow line, boundary conditions in lateral positions were not considered in this investigation. However, as the profile used is situated in the lowest part of Shirase drainage basin, divergent water movement is expected to be small enough to be neglected.

The reconstructed ice surface profile fits well with the measured one when the ice margin is assumed to be 30 km beyond its present position (Fig. 3A). This means that, if we assume the more expanded ice sheet into Lutzow-Holm Bay in the past, and that the ice surface profile was almost the same as the modern one without any thickening of inland ice, then the only difference between the two is a significant thinning of the ice recognized around the outlet of the Shirase Glacier. Mae and Naruse (1978) and Nishio *et al.* (1989) suggested that an increase of the area of basal sliding and an increase in the ice deformation rate can explain thinning of the ice sheet. Regarding recent development in the knowledge of subglacial till deformation (*cf.* Alley, 2000), we should also consider the possibility of

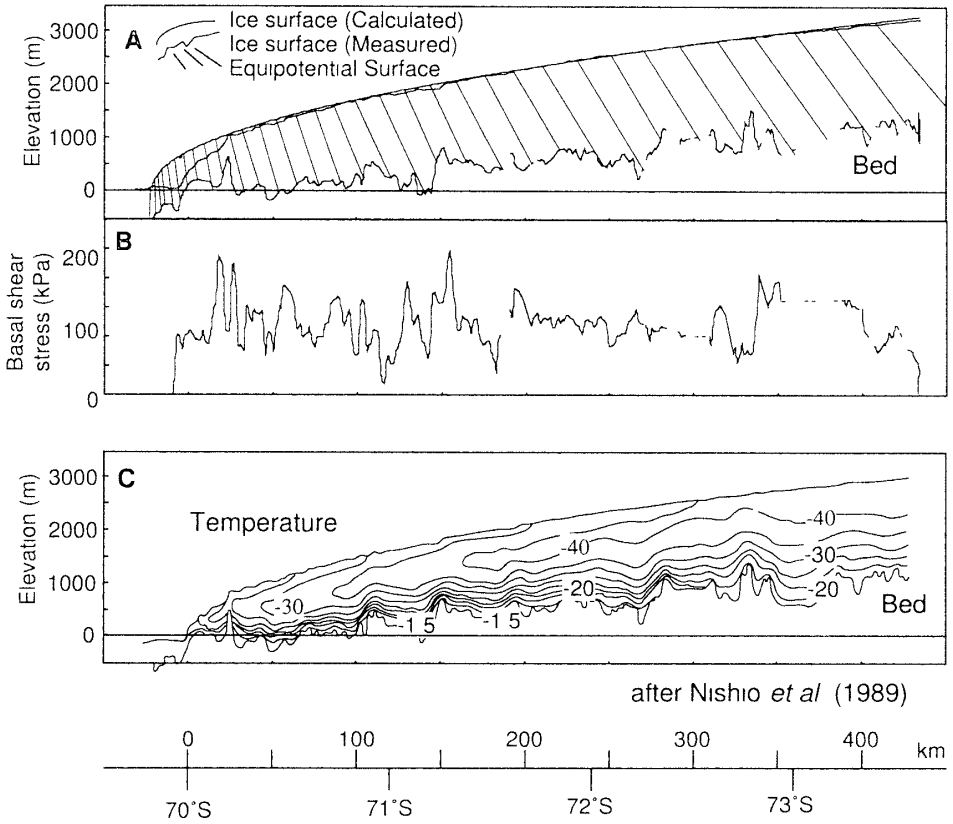

Fig. 3 A. Ice surface profile with bed topography and englacial equipotential surfaces. To simplify the calculation of the englacial equipotential surface, the ice surface profile was reconstructed using the integrated equation of the ice surface profile (see text). B. Basal shear stress profile. C. Temperature profile along the Shirase drainage basin (from Nishio et al., 1989).

increased flow by deformation of subglacial sediments Since a subglacial deformed bed (*cf* Hart, 1998) is not observed beneath the Shirase Glacier, further investigation of its subglacial condition is strongly recommended Thus, we tentatively attribute the modern subglacial conditions to those of the Last Glacial Period

2.4. Possibility of subglacial lakes

Here, we pay attention particularly to the region between the coast and 270 km inland from the ice margin because Nishio *et al* (1989) calculated that the recent basal temperature in that region is at the pressure melting point (Fig 3-C) The detailed equipotential surface within the ice sheet along FL-SG is shown in Fig 4 In this figure, the full water storage condition is represented by an equipotential contour line contacting with the high point of subglacial bed at the downflow side

Accordingly, in the hydrostatic viewpoint, at least fifteen depressions where subglacial water storage is likely to occur are found between the coast and 270 km inland from the

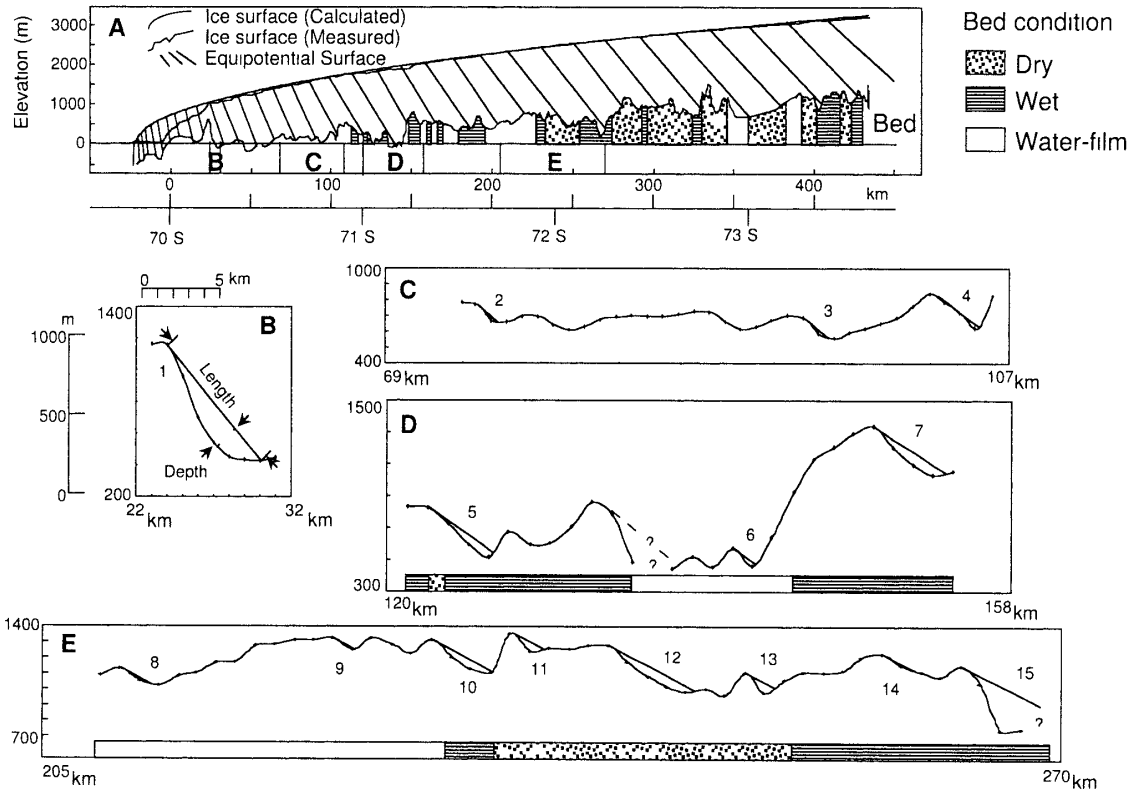

Fig 4 A Calculated equipotential surface within the ice sheet B, C, D, E Inferred subglacial lake surfaces along the Shirase drainage basin with sub-ice condition along the same profile inferred by radio-echo sounding by Ohmae (1988) Subglacial meltwater is expected accumulate in the bed depressions, and water surfaces are determined so as to be the equipotential surfaces A fully water storage condition is represented by an equipotential contour line contacting with the topographic highs of the subglacial bed at the downflow side Its length is determined by that of along the equipotential line, and the depth is determined by the maximum perpendicular distance between this line and the bed (B) These properties of the inferred subglacial lakes are listed in Table 1

Table 1 Properties of the inferred subglacial lakes along the flow line of the Shirase Glacier

No	Vertical cross-sectional area (km^2)	Height (m)	Longitudinal distance (m)	Depth (m)
1	0 904	727	6000	299
2	0 013	111	1300	20
3	0 005	122	1500	6
4	0 005	83	1200	8
5	0 036	289	3800	19
6	0 008	80	1400	12
7	0 060	285	4800	25
8	0 003	90	1500	4
9	0 002	70	1300	3
10	0 063	200	3500	36
11	0 008	102	2000	8
12	0 152	290	6000	51
13	0 011	90	2000	11
14	0 003	110	3000	2
Total area	1 268			

ice margin (Fig 4) Their size ranges from 1–6 km in length and 2–300 m in depth (Table 1) The largest one is situated on the inland-side of the steep mountain 22 km-inland from the coast Its surface extends for 6 km and its depth is calculated to be 300 m Because the possible subglacial basins are seen only 2-dimensionally along the flow line, it is not possible to estimate the exact volume and surface area of the water storage in these basins

Sub-ice thermal conditions inferred by radio-echo sounding by Ohmae (1988) along the same profile are also plotted in Fig 4 This sounding indicates that most of the area between 120 km and 270 km from the outlet of the Shirase Glacier is melting with a small amount of water in the ice mass or a wet-film at the ice-rock interface Judging from the relationship between the inferred subglacial lake locations and the bed condition, there is a high probability of modern subglacial water storage at the sites of basins 5 to 10 In the same way, there is the less probability of subglacial water storage at the other inferred locations at present state

The presence of subglacial depressions does not necessarily mean that they will fill with water Siegert and Ridley (1998) show that there are many of subglacial depressions around Dome C in the vicinity of subglacial lakes, with no lakes within them In fact, there have been no subglacial lakes found in Mizuho Plateau nor beneath Valkyrjedomen Thus, this hydrostatic investigation simply notes the places where some subglacial lakes could have been formed beneath the Shirase Glacier under the right subglacial thermal conditions

3. Modeling of ice sheets and subglacial water flow

3 1 Calculation model of subglacial water flow

In this section, attention is concentrated at a regional scale, concerning the subglacial meltwater erosion of the streamlined bedforms observed in the ice-free areas along the Sôya Coast (Sawagaki and Hirakawa, 1997) As a second investigation, we develop a numeri-

cal model to calculate the subglacial hydraulic potential gradient with special reference to subglacial water flow Using this model, we estimate ice surfaces, which show the conformity of water flow beneath the ice sheet to the underlying bed topography

Shaw (1983) and Kor *et al* (1991) suggested that the distribution of erosional forms of several different scales was controlled by bed topography and the different scales of subglacial water flow structure, with some feedback between the two Concerning their suggestions, we believe that, if there is good conformity between the modelled patterns of subglacial water flow and bedform distribution, then there is a good possibility that meltwater was responsible for the formation of the bedforms As well, the assumed ice surface model is taken to represent the former ice sheet beneath which this erosion took place

Where ground water flow is negligible due to low bed transmittivity, one can reconstruct subglacial water flow on the assumption that the flow is controlled by hydraulic potential gradients beneath the ice mass Thus, the water at the glacier bed need not follow the bed gradient, but instead moves from areas of high hydraulic potential to areas of low potential (Shreve, 1972) Equations (1) and (2) indicate that the control of subglacial water flow by the ice-surface gradient is about 11 times stronger than by the slope of the bed topography Subglacial water flow is generally assumed to flow diagonally down valley sides, or even uphill in the case of beds which slope against the direction of glacier flow (Oswald and Robin, 1973, Hooke, 1989, Sugden *et al*, 1991) Hooke (1989) pointed out that enhanced pressure of ice flowing against the stoss side of a bump distorts the pressure field This dynamic pressure component should be included in equation (1) However, Booth and Hallet (1993) demonstrated that sliding-induced pressure variations can be ignored at all but the smallest scales of individual landforms Consequently, here we do not take into consideration the kinematic pressure field resulting from flow of ice, but assume a static ice sheet Thus, this study includes simplification

Figuer 5 illustrates an ideal example for the numerical modeling of the potential gradient around a bump on a glacier bed In this figure, the bed topography and the ice

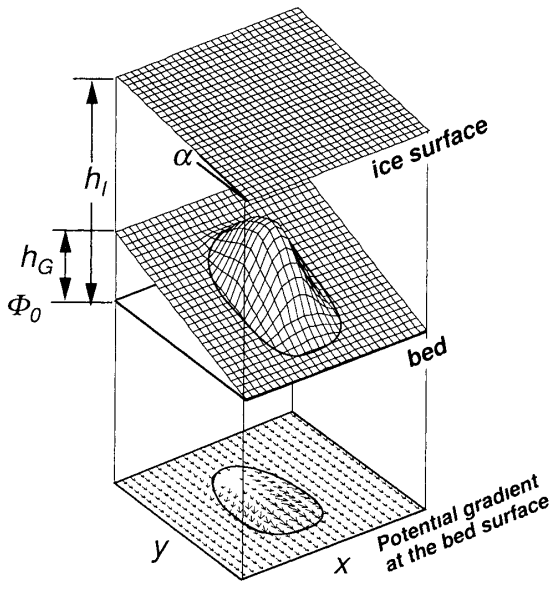

Fig 5 Schematic diagram for the calculation model of potential around a bump on a glacier bed Bed topography and the ice surface were constructed as numeric grid surfaces Calculated potential gradient at the glacier bed in each square grid is indicated by an arrow

surface are indicated as numeric grid surfaces identical with the elevations (h_G, h_I) from a reference potential surface (Φ_O) at their location An ice surface falling parallel to the y-axis with a slope of α is applied in this example The hydraulic potential at the glacier bed was calculated using of eqs (1) and (2) at each grid square The magnitude and direction of the potential gradient in each square are indicated by the lengths and directions of arrows respectively, which are projected onto a map of the bedform distribution The example in Fig 5 indicates that, under proper conditions, subglacial water is expected to flow over the bump rather than around it

3 2 Glacial sculptured bedforms

Topographic features of the ice-free areas along the Sôya Coast are characterized by mammilated peaks and undulating hilly land completely composed of bedrock The distribution of morainic detritus is mainly limited to local depressions behind hillocks (Yoshida, 1983) The bedrock is composed of crystalline gneisses, marble, and calcareous skarn with an E-W or ESE-WNW trending structure (Yoshida *et al*, 1976, Ishikawa *et al*, 1977)

Subglacial sculptured erosion forms are generally better preserved in the ice-free areas along the southern part of the coast (Yoshida, 1983, Sawagaki and Hirakawa, 1997) We identified drumlin-shaped rock hills and small-scale erosional marks (s-forms, Kor *et al*, 1991) The streamlined bedforms in this region are classified into tadpole rocks (Dionne, 1987), transverse ridges (Kor *et al*, 1991), and roches moutonées We argue that the s-forms, tadpole rocks and transverse ridges are best explained by subglacial fluvial erosion (Sawagaki and Hirakawa, 1997)

We concentrated our experimental study on the Skarvsnes and Skallen ice-free areas (Figs 2, 6 and 7) where sculptured erosion forms are well developed The Skarvsnes district is the largest ice-free area along the coast It juts into the sea to the west and is bounded to the east by the ice sheet The area is 64 km^2 and the elevation ranges between 40 m below sea level and 400 m above sea level The Skallen district is a relatively small ice-free area of about 14 km^2 in the south of the Skarvsnes district (Fig 7) The ice sheet terminates on the southern edge of this district The eastern coastline faces onto the floating tongue of the Skallen Glacier

More than 2600 streamlined bedforms were identified in Skarvsnes (Sawagaki and Hirakawa, 1997) In some cases larger forms have been modified by the formation of smaller, superimposed forms on the crest and flanks Typical bedforms in Skarvsnes are crescentic transverse ridges and streamlined hills with the steeper slope facing up-ice (tadpole rock) Longitudinal troughs parallel to the tadpole rocks form furrows They appear on airphotos as a fluting pattern, 10–1000 m long, 1–30 m wide, and up to 10 m deep (Fig 6) Some superimposed tadpole rocks were recognized on the southeastern flank of the stoss slope of Mt Suribati on the central part of this district, which forms a particularly large roche moutonnée, about 250 m high with a gentle abraded slope on the upstream side and cliffs with talus slopes on the downstream side (Fig 6) At the local scale, crescentic transverse ridges are commonly accompanied by stoss-side furrows which indicate the up-ice side of the ridges (Kor *et al* 1991, Sawagaki and Hirakawa, 1997) Glacial striae marked on the bed surface are oriented E-W in the area of Fig 6

In Skallen, the long axes of the streamlined hills show two distinctive directions, E-W

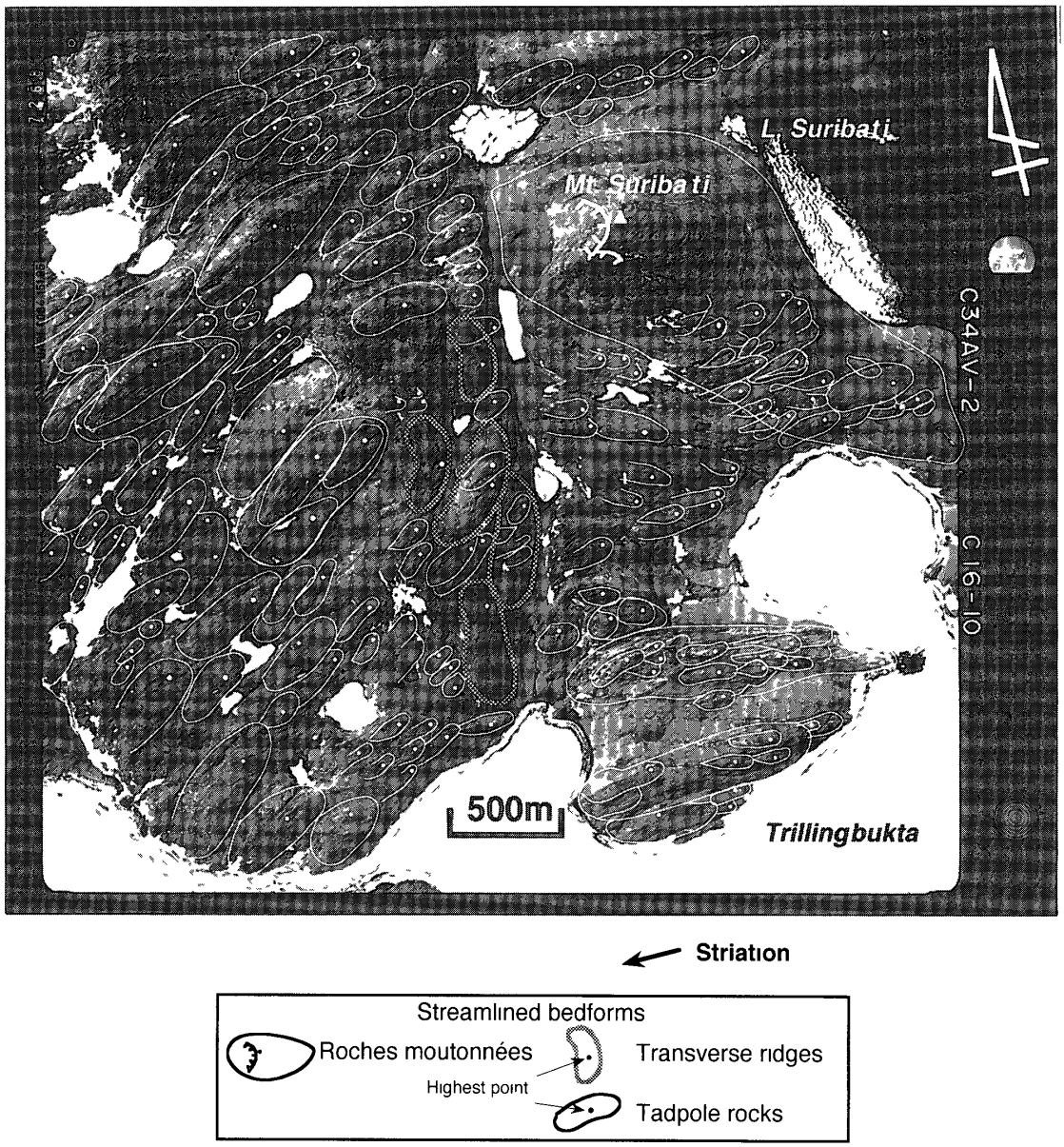

Fig 6 Distribution of the streamlined bedforms in Skarvsnes (after Sawagaki and Hirakawa, 1997) Outlines of the bedforms are projected onto a topographic map of this region Indicated area is same the area of Fig 8-A

and ESE-WNW (Fig 7) The E-W trending forms have smaller ESE-WNW trending forms superimposed upon them Glacial striae marked on the bed surface are oriented S-N, ESE-WNW and SE-NW The topography in Skallen is rather smooth and of low-relief, and the streamlined hills in this area do not show distinctive stoss-and-lee forms However, they are clearly distinguished from transverse ridges in Skarvsnes, because no stoss-side furrows are observed on them, and individual hillocks are separated by troughs such as arms of sichelwanne and comma-forms (Kor, *et al*, 1991) elongated from the eastern side of the hills (Sawagaki and Hirakawa, 1997)

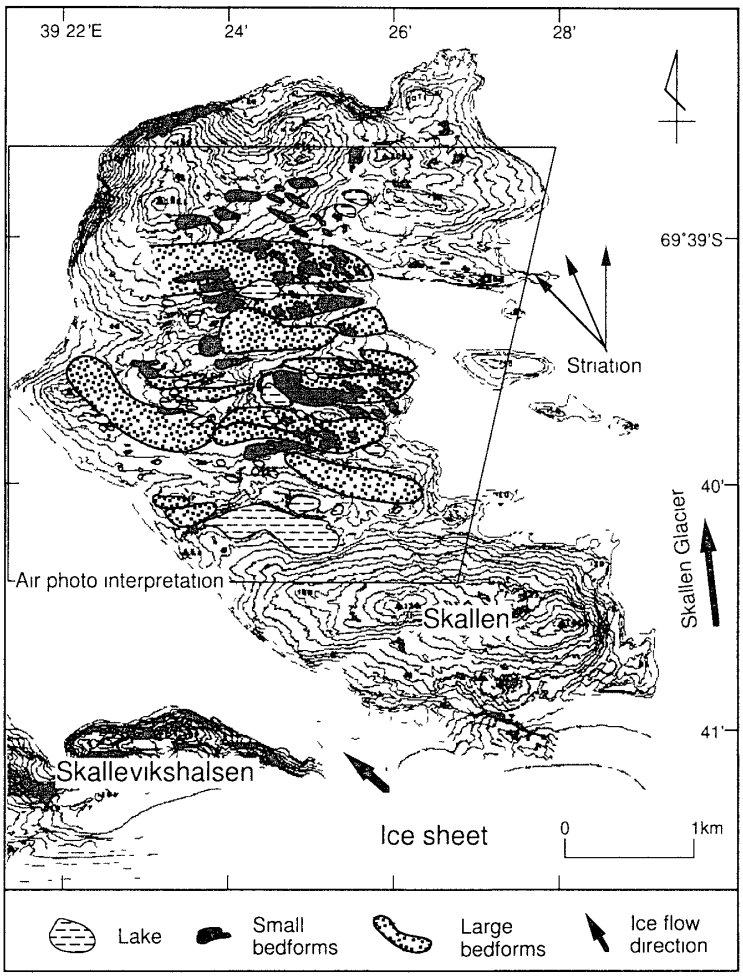

Fig 7 Distribution of the streamlined bedforms in Skallen (after Sawagaki and Hirakawa, 1997) Outlines of the bedforms are projected onto a topographic map of this region Indicated area is same the area of Fig 8-B

3 3 Data collection

Two reconstructed elements, bed elevations and the ice surface, are required to calculate the hydraulic potential gradient at the bed A topographic map of the south central part of Skarvsnes at a scale of 1 5000 with 10 m contour intervals, and a topographic map of Skallen at a scale of 1 25000 with 10 m contour intervals were used Present-day ground elevations were collected from intersection points of a square grid superimposed on the topographic maps, with a 50 m mesh in Skarvsnes (Fig 8-A) and with a 100 m mesh in Skallen (Fig 8-B) The sample area in Skarvsnes extends about 3 5 km east-west and 2 5 km north-south, and in Skallen it extends about 4 5 km east-west and 4 5 km north-south These mesh intervals and areas were determined based partly on the capability of a data processor we used, and partly on the required scale effect, discussed by Booth and Hallet (1993), if the sliding-induced pressure variations are to be ignored The bedrock surface is determined for the whole area, except beneath lakes and sea where the bathymetry is unknown Thus calculations for the presently water-filled areas are unavailable

In order to obtain the exact position of the streamlined bedforms in both areas, the

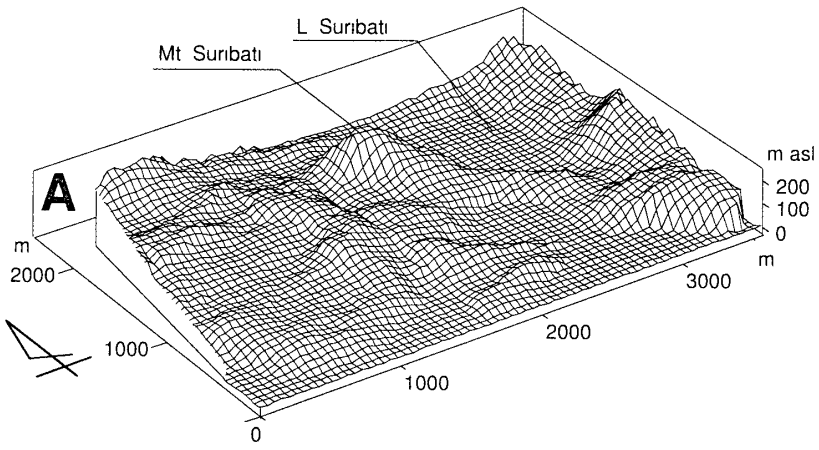

Fig 8 Block diagrams of the present-day surface topography of the calculated areas in Skarvsnes (A) and Skallen (B) Vertical exaggeration is 1 3

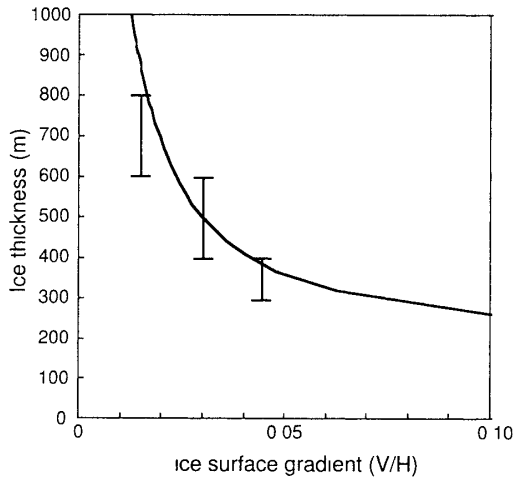

Fig 9 Relation between ice surface gradient and ice thickness derived from the ice surface profile determined by equation (5) Inner bars indicate the ice surface gradients of the averaged ice-surface profile at the present state of the ice margin along the Sôya Coast

outlines of these forms were projected onto topographic maps using the color air photos with the Analytical Photogrammetric System (Figs 6 and 7)

Theoretically, an ice surface profile is approximated by eq (5), and the relation between ice surface gradient and ice thickness derived from the ice-surface profile by eq (5) is shown in Fig 9 However, the exact position of the ice sheet terminus and the ice divide in the course of its retreat is uncertain In addition, the surface profile of ice is much more variable near the terminus than in the central part of an ice sheet Thus, we assume that the most probable ice sheet took part in the development of the bedforms extended to the western edge of the present ice-free areas flowing perpendicular to the coast Secondly we assume that the marginal ice surface profile at that time was similar to the shape of the present-day ice surface profile near the ice margin We use the averaged ice-surface profile at present state of the ice margin along the Sôya Coast for the calculation, its ice-surface gradients are 0 045 between 300–400 m in ice thickness, 0 030 (400–600 m thick), and 0 015 (600–800 m thick), respectively These values are also indicated in Fig 9, and the relations seem to be fit well to the theoretical approximation Thirdly, since the investigated areas extend 4 5 km at most, we think that a planar ice surface is assumable for such small scales

According to these assumptions, a number of ice surface elevation models of various ice surface gradients and down-slope directions are reconstructed for the calculation

3 4 Conformity between the potential gradients and the bedform distribution

Calculations of subglacial potential gradients were made assuming several different ice surface models in Skarvsnes and Skallen The results indicate that the potential gradients generally trend in the same direction as the ice-surface gradient When the ice surface gradient is steep, the subglacial water is much more likely to flow uphill following the direction of this gradient However, the direction of the subglacial hydraulic potential changes regionally with the underlying topography because the bedrock elevation also

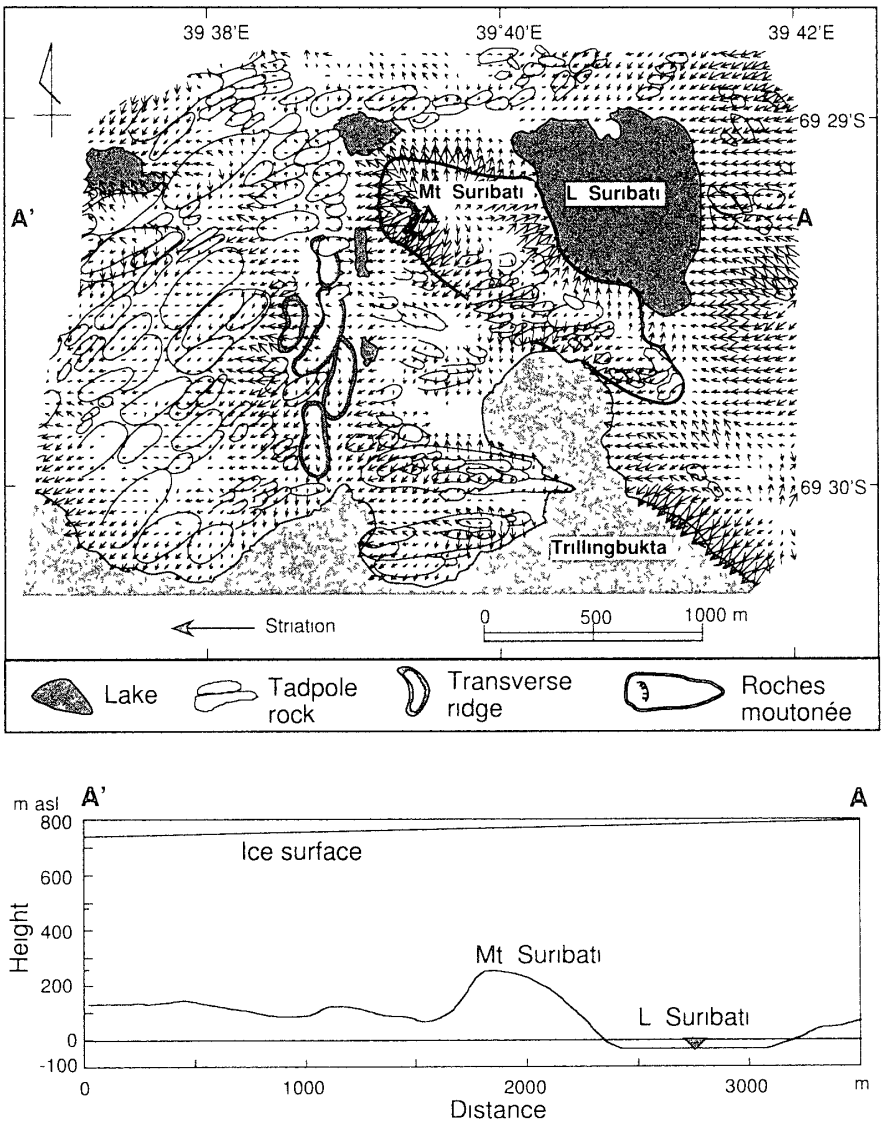

Fig 10 Simulation of hydraulic potential gradients below the ice sheet terminus in Skarvsnes Ice surface is assumed to be of an inclination of 0 015 from east to west (A to A') Arrows of the potential gradient are plotted with the distribution of streamlined bedforms (upper), and a longitudinal section along the maximum ice surface gradient showing the bed topography and the inferred ice surface (lower)

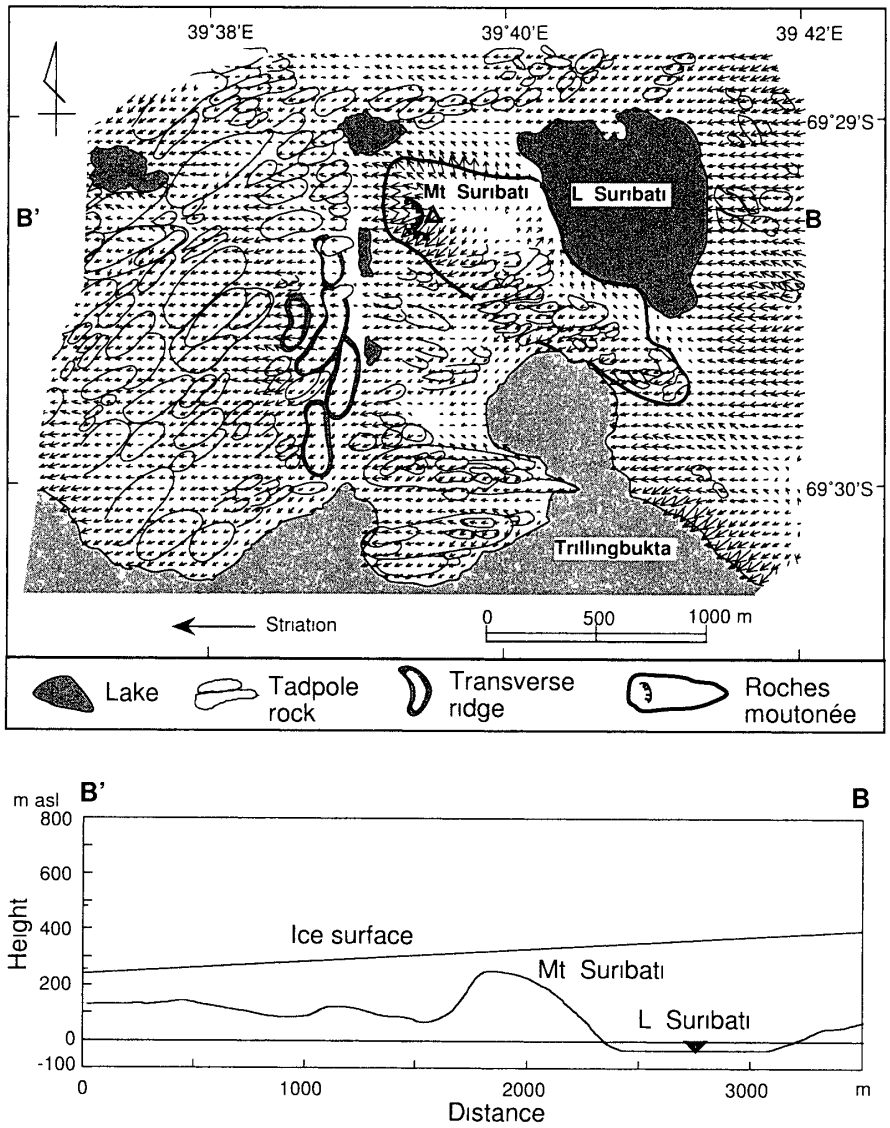

Fig 11 Simulation of hydraulic potential gradients below the ice sheet terminus in Skarvsnes Ice surface is assumed to be a slope of 0 045 from east to west (B to B')

helps determine the potential Thus, to find the best match between the potential gradients and the bedform distribution, a number of the ice-surface models were tried iteratively (3 ice surface gradients with 16 azimuths) Figures 10, 11 and 12 show three examples of the iterative approach used to estimate the former ice-surface slope in the southern central part of Skarvsnes

In Figs 10 and 11, we assumed two ice surfaces falling from E to W at different slopes As has been assumed above, this westerly sloping ice surface is chosen because it mimics the recent westward ice flow direction perpendicular to the coast The orientation of glacial striations in this area also support this assumption We believe that these glacial striae were formed by direct glacial erosion, not by subglacial water However, these erosional marks would also represent the ice-flow directions at the water discharge events, because subglacial water events would have been short lived without significant change in ice flow direction (Shoemaker, 1991, 1992a, b, Shaw, 1996)

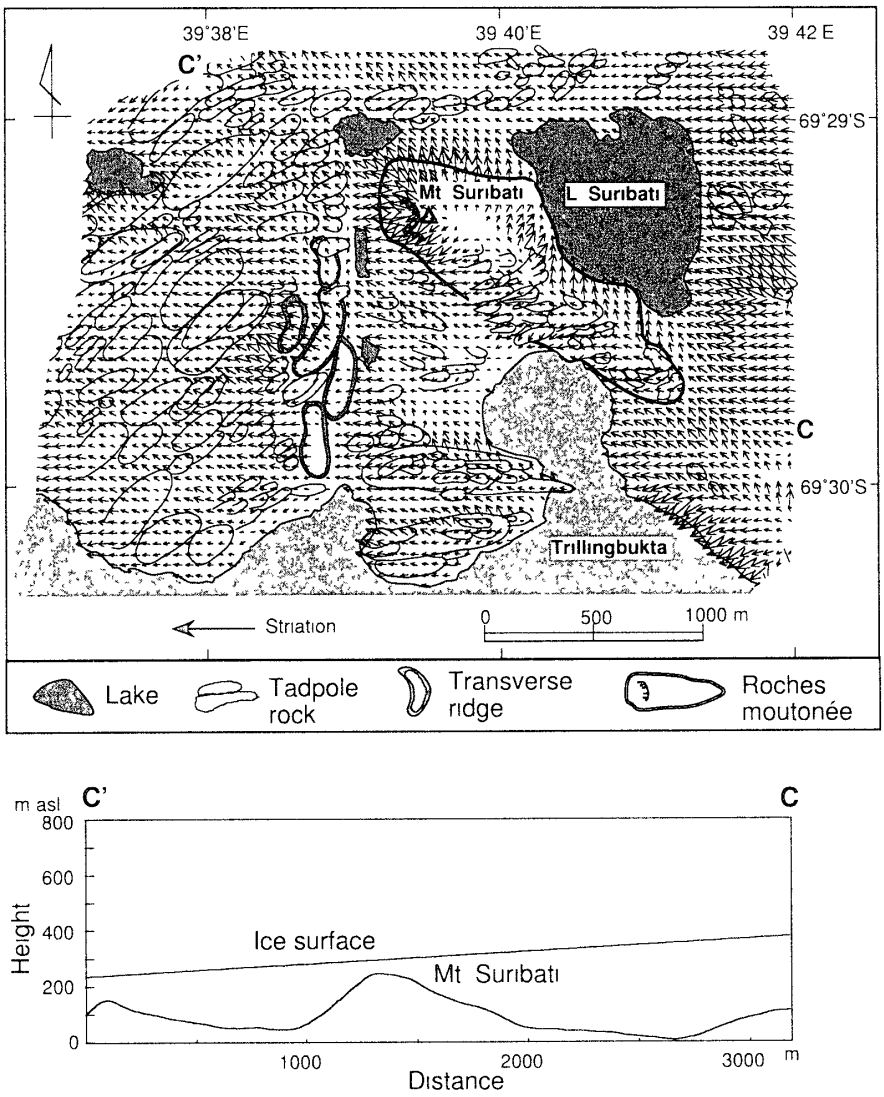

Fig 12 Simulation of hydraulic potential gradients below the ice sheet terminus in Skarvsnes Ice surface is assumed to be a slope of 0 045 from ESE to the WNW (C to C')

When an ice surface gently sloping 0 015 is assumed for the modeled areas (Fig 10), the ice thickness is assumed to be about 800 m (Fig 9) In this model (Fig 10), the arrows tend to point downslope parallel to the bed topography but against the direction of the ice surface gradient, especially on the stoss side of the bedforms By contrast, in the case of an ice surface sloping at 0 045 (the assumed ice thickness is about 400 m) the flow shows a much closer conformity to the topography (Fig 11) Several significant trends of the potential gradient were recognized in the model of Fig 11 Those are 1) potential gradients in the vicinity of Mt Suribati are either over the top or around the mountain, 2) potential gradients on the flanks are parallel to the long axes of the superimposed tadpole rocks, and 3) the potential gradients to the west of Mt Suribati are across transverse ridges Given the above conformity of the flow and topography, we determined that the model of Fig 11 applies at Skarvsnes

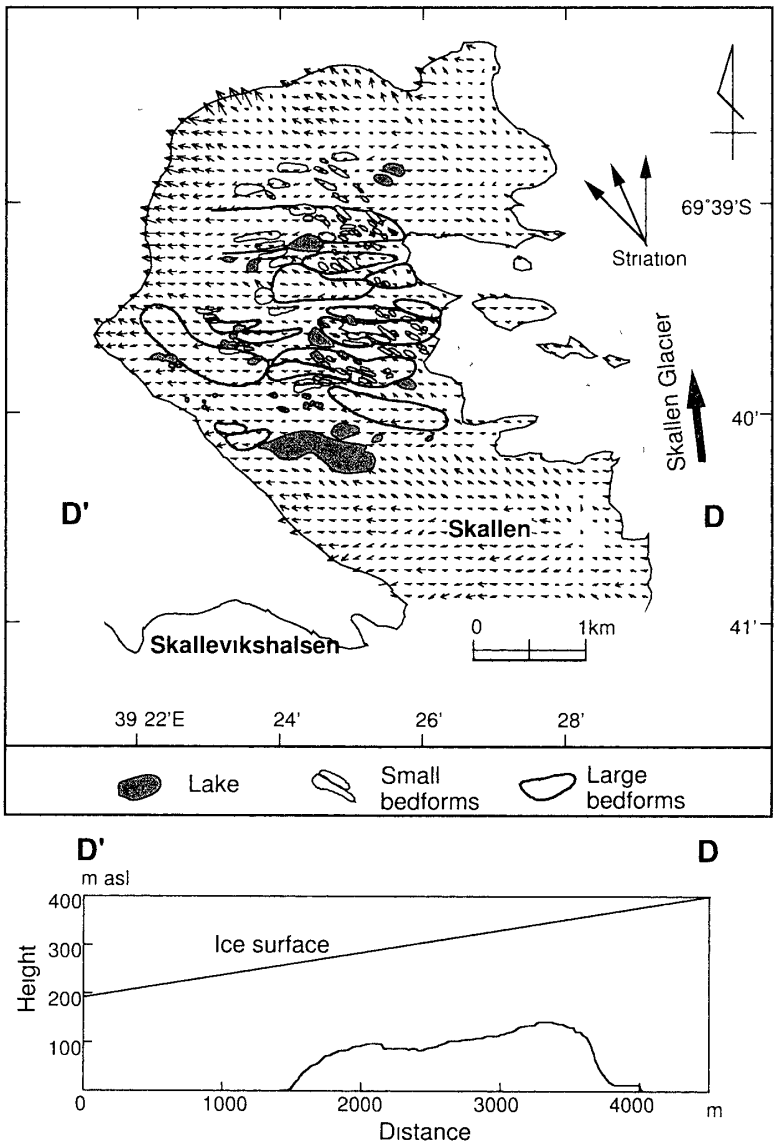

Fig 13 Simulation of hydraulic potential gradients below the ice sheet terminus in Skallen Ice surface is assumed to be a slope of 0 045 from east to west (D to D')

As an additional example to show the iteration, we assumed an ice surface falling from ESE to WNW with the same slope and ice thickness as Fig 11 of 0 045 and 400 m thick (Fig 12) Since no glacial geological evidence indicating an ice flowed from ESE to WNW has been obtained in this area, this model seems unlikely For this model, the arrows tend to point WNW, but the regional variation of the arrows is not in agreement with the topography, especially in the western part (Fig 12)

The iterative approximation of the ice surface in Skallen is more difficult than in Skarvsnes, because the relief in this region is not so steep as to affect the potential gradient beneath the ice In particular, the subglacial water flood flowing over the hills occurs even beneath an ice sheet with a gentle surface slope We thus used an ice surface slope of 0 045 (the assumed ice thickness is about 400 m), the same as for Skarvsnes The potential gradient was calculated using three different ice surface models one from E to W (Fig 13),

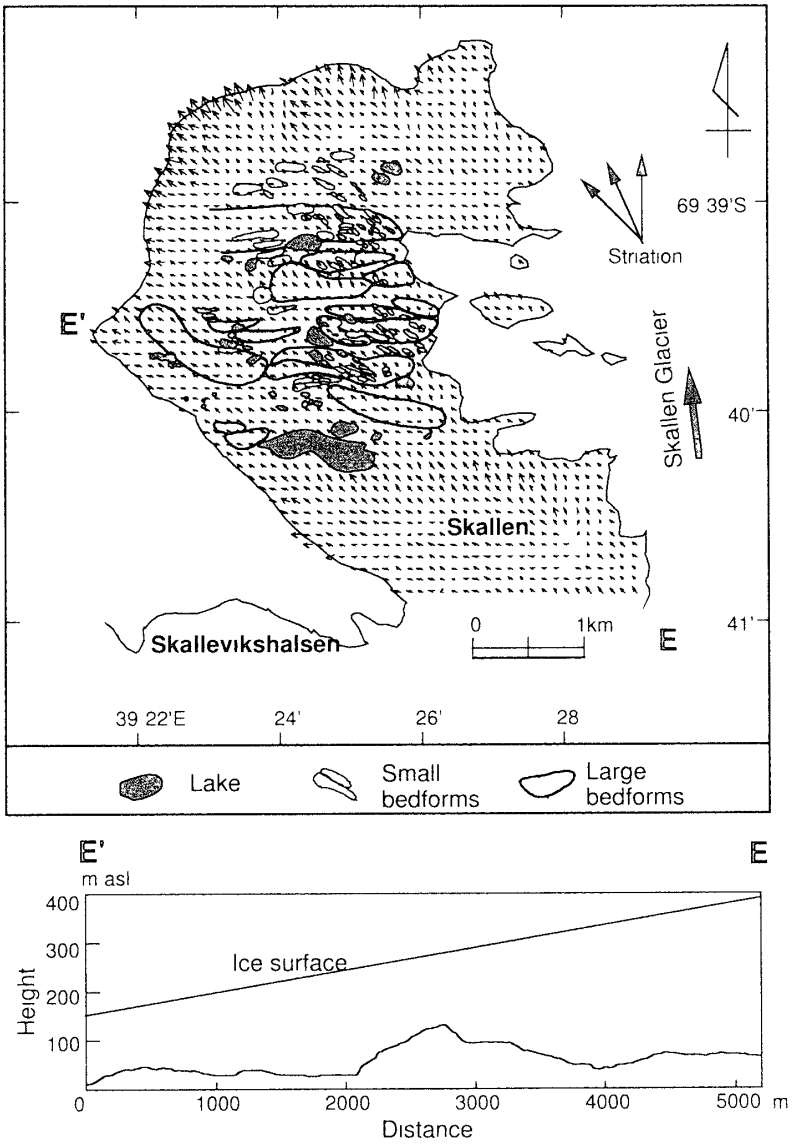

Fig 14 Simulation of hydraulic potential gradients below the ice sheet terminus in Skallen Ice surface is assumed to be a slope of 0 045 from ESE to WNW (E to E')

one from ESE-WNW (Fig 14), and a third from S-N (Fig 15) The first flow direction is the same as the successful model in Skarvsnes, and the latter two were chosen based on the directions of glacial striae on the bed

The case where the ice surface slopes WNW (Fig 14) shows the best conformity to both the larger streamlined bedforms and smaller superimposed ones While, the case where ice surface slopes to the north (Fig 15) does not seem to produce flow lines conformable to any landforms Using a westward slope (Fig 13), some flows conform with the larger bedforms, but this model is not as successful as the one with a WNW ice slope

3 5 Suggested development of the landforms

Sawagaki and Hirakawa (1997) presented an idea that there are two kinds of glacial

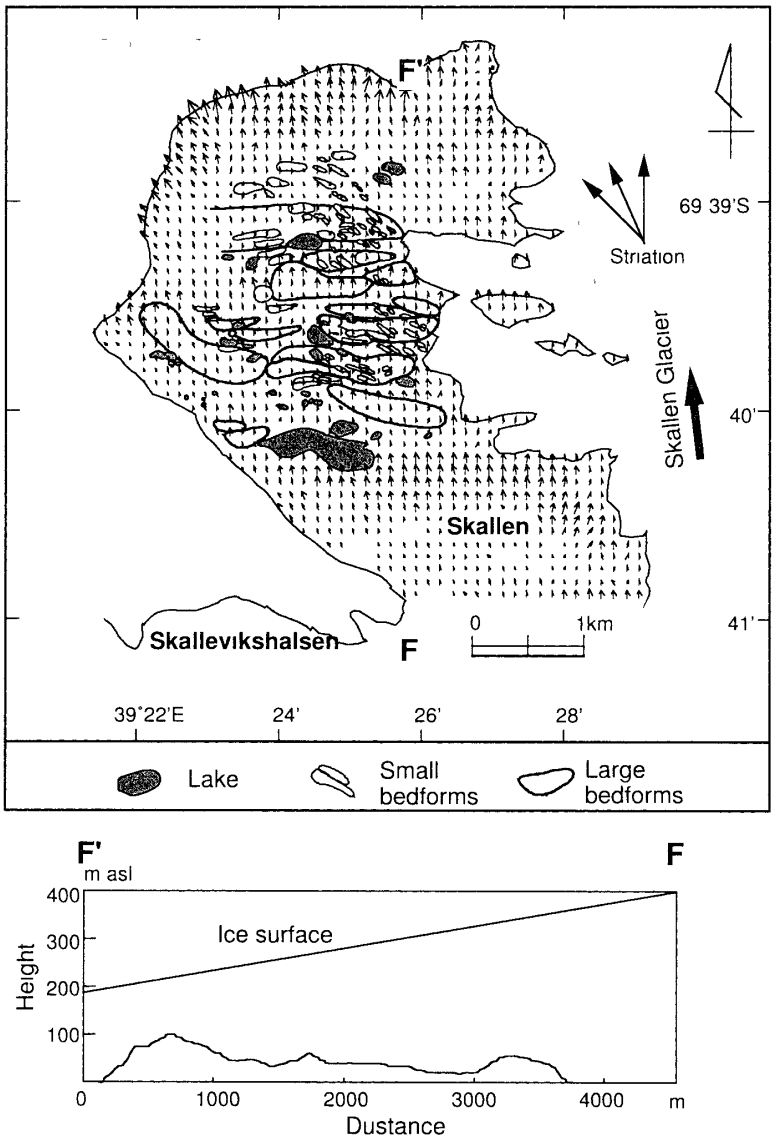

Fig 15 Simulation of hydraulic potential gradients below the ice sheet terminus in Skallen Ice surface is assumed to be a slope of 0 045 from south to north (F to F')

erosional features in the study area One is the product of glacial abrasion and plucking beneath a wet-based ice sheet These forms include glacial striae and roche moutonnée The other kind are the streamlined bedforms, to which we apply the above theoretical examination of subglacial water flow By applying the results of the calculations to the interpretation of Sawagaki and Hirakawa (1997), we infer the change of ice flow direction and the evolution of basal processes

As is shown by the calculations, a single ice-surface model gives rise to potential gradients conformable with the topography in Skarvsnes Since local water flow, controlled by the large-scale bed topography, converged towards the southern flank of Mt Suribati, the superimposed tadpole rocks are concentrated on the southern flank of this mountain Thus, interpreted as a large roche moutonnée, Mt Suribati could be seen as an earlier product of abrasion and plucking with superimposed tadpole rocks Because

subglacial water events would have been short lived (Shoemaker, 1991, 1992a, b, Shaw, 1996), we suggest that subglacial water erosion occurred as a short interruption of continuous glacial abrasion by the ice flowing westward Accordingly, it is suggested that both glacial abrasion forms and subglacial water flow forms in this region were sculpted without significant change of the ice-surface profile

The calculation reveals two conformable ice-surface models in Skallen, with one surface inclined westward for the larger bedforms, and the other inclined northwestward for both the larger and smaller bedforms Based on these results, the glacial flow direction changed from westward to northward Sawagaki and Hirakawa (1997) presented four stages in development of the bedforms 1) large-scale glacial plucked and abraded bedforms in Skarvsnes (possibly in Skallen) (stage-1), 2) large-scale and E-W trending streamlined bedforms formed by subglacial water flow in Skarvsnes and Skallen (stage-2), 3) superimposition of ESE-WNW trending small-scale forms in response to subglacial water flow in Skallen (stage-3), and 4) superimposition of northward striations upon in response to local ice flow in Skallen (stage-4) As has been suggested in this sequence, glacialy plucked and abraded features of stage-1 are not observed in Skallen The calculations of this study readily suggest that glacial plucked and abraded forms in Skallen were modified and removed as subglacial meltwater erosion formed streamlined debforms in stage-2 Consequently, we think that the reconstructed ice-surface models in Skallen represent those of stages 2 and 3 in Sawagaki and Hirakawa (1997) These reconstructed ice-surfaces may indicate transitional states of the ice sheet to local ice flow conditions of the Skallen Glacier

5. Discussion

What type of ice sheet would form subglacial lakes? And what would have happened had such subglacial water flooded into the ocean? Unfortunately, we do not have any further information to answer this question, such as an exact ice surface profile, subglacial bed conditions, or thermal regime of the ice sheet in the past The only way to proceed is by way of inductive estimation of the palaeo-ice sheet using terrestrial and glacial geological features observed in the ice-free areas along the Sôya Coast, and recent knowledge on the melting history of the Antarctic Ice Sheet and the global response of oceans

5 1 Hydrostatic implication for subglacial outburst flood

In the references to modern Antarctic subglacial lakes, there are several subglacial lakes reported near to the initiating regions of ice streams (cf Siegert *et al*., 1996, Dowdeswell and Siegert, 1999, Siegert, 2000) Such subglacial lakes are likely to be involved in outburst floods since they would have the benefit of a warm-based pathway beneath the ice stream to the proglacial region The hydrostatically estimated depressions in this study also benefit from this condition along FL-SG

Water is produced subglacialy by geothermal and frictional heat where the ice temperature is at pressure melting point According to the previous glaciological studies, the rate of water produce beneath an ice sheet is generally expected to be a few mm/yr (cf Shaw *et al*, 1989, Shoemaker, 1991, 1992a, b, Kapista *et al*, 1996) As already stated,

Nishio *et al* (1989) calculated that the basal temperature along the Shirase drainage basin is at pressure melting point between 20 km and 260 km from the coast Nevertheless, as the exact geothermal heat flux along this basin is not known, remains it difficult to estimate the actual melting rate in the studied area

Setting aside the question of the melting rate, in the hydrostatic view point, we will consider evacuating systems in which a large amount of subglacial water might have been evacuated to the ice margin At first, once the subglacial meltwater has been produced, the water first fills the nearest subglacial basin When the upper basins were filled by water, the subglacial water spilled to the next lower basin or to the ice margin Once fully ponded conditions had been established, steady-state drainage occurred However, it is unlikely that a steady-state subglacial drainage system is permanent because there is insufficient pressure gradient to sustain flows over some hundreds of kilometers (Shoemaker, 1991) Even if the steady-state drainage existed, discharges from such system are not sufficient to sculpture bedrock on a regional scale Consequently, other evacuating systems for subglacial meltwater thus should be considered to meet the requirement

As has been indicated by the first investigation, the size of the subglacial basin is controlled mainly by the overriding ice-surface topography, since the bed topography has been unchanged This means that the gradient of the englacial equipotential surface changes in response to ice-sheet fluctuation For example, when the ice expanded further than today, the ice-surface gradient at a point would have been gentler than now, which would have reduced the slope of the equipotential surface In the course of deglaciation or thinning of ice sheet, the ice-surface gradient at a point steepens, particularly near the ice margin Owing to this steepening, equipotential surfaces within the ice also steepens, making subglacial basins smaller and shallower In response to the shrinkage of subglacial lakes, excessive water must be evacuated to the terminus, otherwise the ponded water should be more highly pressured

Although it is hard to imagine the above process occurring quickly enough to cause the sudden outburst because the slope changes during retreat would have been slow, more effective triggering would be possible when ice floats on the high-pressured, ponded water Another effective trigger would be possible where ice is frozen to the bed downflow of a subglacial depression, because such subglacial ice dams would be easily collapsed by melting or hydrofracturing of ice to release the accumulated water Subglacial flooding should be generated by such breaching of ice dams to evacuate water through englacial or subglacial tunnels, and the tunnel flow should evolve into a sheet-flow near the ice margin to form the spatially distributed streamlined bedforms

5 2. Timing of the subglacial water discharge

Sawagaki and Hirakawa (1997) suggested in an initial investigation that the ice-free areas along the Sôya Coast once experienced subglacial water erosion There is no direct dating showing when the glacial and subglacial water erosional forms were created However, we think that the fine preservation of the eroded bedforms along the Sôya Coast indicates formation during the last major geomorphic activity of the Antarctic Ice Sheet Based on this assumption and other terrestrial evidence derived from the Sôya Coast region, the timing of the subglacial meltwater event is discussed below together with a review of past ice sheet features

Hayashi and Yoshida (1994) suggested that the ice sheet covering the present ice-free areas was not thick during the Last Glacial Maximum (LGM), and this ice retreated from the coastal areas prior to 35 kyr BP Their conclusions are based on the Late Quaternary marine limit in this region, which is a reflection of the regional isostatic rebound Coinciding with this implication, we provisionally assumed in our second qualitative model that the ice sheet had extended to the western edge of the recently deglaciated areas The assumed ice thickness is about 400 m for the modeled areas Once a suitable ice-surface model was determined by trial-and-error, a strong conformity between estimated hydraulic gradients and the bedform distribution was obtained We argue that the conformable ice-surface model represents the former ice sheet that took part in the morphological development of the hills, and that the subglacial water flow could have been short lived without involving significant change of the ice-surface profile

If subglacial outburst floods occurred, they may have been massive enough to leave a signal in the global climate record (Blanchon and Shaw, 1995) Based on the low oxygen isotopic ratio of fossil shells and the occurrence of fluvial sediment intercalated in the raised marine sediments along the Sôya Coast, Miura *et al* (1998) pointed out that considerable melting of the East Antarctic Ice Sheet occurred during the period 30–46 kyr BP (Marine Isotope Stage 3) Recently, the cause of a massive and unusually abrupt rise in sea level about 14 kyr BP, called the global meltwater pulse (MWP, Fairbanks, 1989), has been discussed Clark *et al* (2002) suggested that MWP-IA was caused by the partial collapse of the Antarctic Ice Sheet Yokoyama *et al* (2000, 2001) also discovered a meltwater pulse which was caused by a rapid decrease in ice volume within a few hundred years, terminating the LGM at about 19000 cal-yr BP We present an idea that a combination of water accumulation beneath the ice sheet and discharge of this water could make the ice sheet unstable leading to the rapid melting This implies a huge amount of meltwater to the ocean and formation of local ice streams In addition, we tentatively suggest that subglacial meltwater events occurred during MIS-3 or post-LGM periods, which might contribute these MWP events

6. Conclusions

Hydrostatic examination along a flow line of the Shirase Glacier, East Antarctica revealed that several subglacial lakes may have formed in bed depressions with the water surfaces determined by englacial equipotential surfaces Possible subglacial lakes are estimated to have been 1–6 km in length and 200–300 m in depth

Theoretical calculations of water flow beneath the Antarctic Ice Sheet were performed to investigate the distribution of the streamlined bedforms on the ice-free areas along the Sôya Coast The results of the calculations indicate good agreement of potential gradients to the bedform distribution when a suitable ice surface model is obtained As a whole, the assumed ice surface models probably indicate former ice sheet which took part in the erosion of the subglacial water flow

The observed subglacial meltwater erosional forms are thus due to a short-lived subglacial water sheet flood and pre-existed topography The results also support our assumption that the former ice sheet extended to the western edge of the present ice-free areas along the Sôya Coast Subglacial water discharge is supposed to occur in response

to the shrinkage of subglacial lakes and to collapsing of the subglacial dam with some effective triggering phenomena We present an idea that a combination of water accumulation beneath the ice sheet and discharge of this water could make the ice sheet unstable leading to rapid melting supplying huge amount of meltwater to the ocean and the creation of local ice streams It is tentatively suggested that subglacial meltwater events occurred during MIS-3 or post-LGM periods

These attempts add numerical results to the existing set of facts used in the inductive reasoning of the subglacial hydraulic hypothesis However, other direct attempts complete the inventory of Antarctic subglacial lakes and to reveal subglacial bed condition are strongly recommended for the reconstruction of ice sheet fluctuations in Mizuho Plateau

Acknowledgments

We would like to acknowledge the members of the 33rd, 34th and 35th Japanese Antarctic Research Expeditions for their kind collaboration in the field Also, we thank Y Yoshida, K Moriwaki, H Miura, R Naruse, and Y Kurashige for their encouragements and helpful suggestions We thank P Berkman, J Shaw, J T Teller, and D Zwartz for their sincere advice for improving this paper especially its English We also gratefully acknowledge the constructive criticism of anonymous reviewers

References

Alley, R B (2000) Continuity comes first recent progress in understanding subglacial deformation Deformation of Glacial Materials, ed by A J Maltman *et al* 171-179 (Geological Society, London, Special Publications, 176)

Blanchon, P and Shaw, J (1995) Reef drowning during the last deglaciation Evidence for catastrophic sea-level rise and ice-sheet collapse Geology, **23**, 4-8

Booth, D B and Hallet, B (1993) Channel networks carved by subglacial water Observations and reconstruction in the eastern Puget Lowland of Washington Geol Soc Am Bull, **105**, 671-683

Boulton, G S (1974) Processes and patterns of glacial erosion Glacial Geomorphology, ed by D R Coates Binghamton, State University of New York, 41-87 (Publications of Geomorphology)

Boulton, G S (1979) Processes of glacier erosion on different substrata, J Glaciol, **23**, 15-37

Boulton, G S and Hindmarsh, R C A (1987) Sediment deformation beneath glaciers rheology and glacial consequences J Geophys Res, **92B**, 9059-9082

Clark, P U, Mitrovica, J X, Milne, G A and Tamisiea, M E (2002) Sea-Level fingerprinting as a direct test for the source of global meltwater pulse IA Science, **295**, 2438-2441

Dardis, G F and McCabe, A M (1994) Subglacial processes, sediments and landforms-an introduction Sediment Geol, **91**, 1-5

Dionne, J C (1987) Tadpole rock (rocdrumlin) A glacial stream moulded form Drumlin Symposium, ed by J Menzies and J Rose Rotterdam, A A Balkema Publ, 149-159

Dowdeswell, J A and Siegert, M J (1999) The dimensions and topographic setting of Antarctic subglacial lakes and implications for large-scale water storage beneath continental ice sheets Geol Soc Am Bull, **111**, 254-263

Fairbanks, R G A (1989) 17000-year glacio-eustatic sea level record influence of glacial melting rates on the Younger Dryas event and deep-ocean circulation Nature, **342**, 637-642

Hart, J K (1998) The deforming bed/debris-rich basal ice continuum and its implications for the

formation of glacial landforms (flutes) and sediments (melt-out till) Quat Sci Rev, **17**, 737-754

Hayashi M and Yoshida, Y (1994) Holocene raised beaches in the Lutzow-Holm Bay region, East Antarctica Mem Natl Inst Polar Res Spec Issue **50**, 49-84

Hindmarsh R C (1998a) The stability of viscous till sheet coupled with ice flow, considered at wavelengths less the ice thickness J Glaciol, **44** 285-292

Hindmarsh R C (1998b) Drumlinization and drumlin-forming instabilities viscous till mechanisms J Glaciol **44** 293-314

Hooke, R L (1989) Englacial and subglacial hydrology A qualitative review Arct Alpine Res **21**, 221-233

Ishikawa, T Yanai K, Matsumoto Y, Kizaki, K, Kojima, S, Tatsumi T Kikuchi, T and Yoshida, M (1977) Geological map of Skarvsnes Antarctica, Explanatory text Antarctic Geological Map Series Sheet 6 & 7 Tokyo, National Institute of Polar Research

Kapista, A P, Ridley, J K, Robin, G de Q, Siegert, M J, and Zotikov I A (1996) A large deep freshwater lake beneath the ice of central East Antarctica Nature, **381**, 684-686

Koi, P S G Shaw, J and Sharpe D R (1991) Erosion of bedrock by subglacial meltwater, Georgian Bay, Ontario A regional view Can J Earth Sci, **28**, 623-642

Mae, S and Naruse, R (1978) Possible cause of ice sheet thinning in the Mizuho Plateau Nature **273**, 291-292

Menzies, J and Rose, J (1989) Subglacial Bedforms-an introduction Sediment Geol, **62**, 117-122

Miura H, Maemoku, H, Seto, K and Moriwaki, K (1998) Late Quaternary East Antarctic melting event in the Sôya Coast region based on stratigraphy and oxygen isotopic ratio of fossil molluscs Polar Geosci, **11**, 260-274

Naruse, R and Shimizu, H (1978) Flow line of the ice sheet over Mizuho Plateau Mem Natl Inst Polar Res, Spec Issue **7**, 227-234

National Institute of Polar Research (1997) Antarctica East Queen Maud Land-Enderby Land Glaciological Folio, Tokyo

Nishio F, Mae, S, Ohmae, H, Takahashi S, Nakawo, M and Kawada K (1989) Dynamical behavior of the ice sheet in Mizuho Plateau East Antarctica Proc NIPR Symp Polar Meteorol Glaciol, **2**, 97-104

Ohmae H (1988) Radio-echo studies on the sub-ice conditions of the Antarctic ice sheet Doctoral dissertation of Hokkaido University

Oswald G K and Robin G de Q (1973) Lakes beneath the Antarctic Ice Sheet Nature, **245** 251 254

Sawagaki, T and Hirakawa, K (1997) Erosion of bedrock by subglacial meltwater, Sôya Coast East Antarctica Geograf Ann **79A**, 223-238

Sawagaki T and Hirakawa, K (1998) The problem of drumlin formation and glacial geological reconstruction of sub-ice-sheet environments deformation of subglacial sediments or subglacial floods? J Geogr, **107**, 469-492 (in Japanese with English abstract)

Shaw J (1983) Drumlin formation related to inverted melt-water erosional marks J Glaciol, **29**, 461-479

Shaw, J (1996) A meltwater model for Laurentide subglacial landscapes Geomorphology Sans Frontieres ed by S B McCann and D C Ford New York, J Wiley, 181-236

Shaw, J (2002) The meltwater hypothesis for subglacial bedforms Quat Int, **90** 5-22

Shaw, J Kvill, D and Rains, B (1989) Drumlins and catastrophic subglacial floods Sediment Geol, **62**, 177-202

Shimizu, H, Yoshimaru, A, Naruse, R and Yokoyama, K (1978) Morphological feature of the ice sheet in Mizuho Plateau Mem Natl Inst Polar Res, Spec Issue, **7** 14-25

Shoemaker, E M (1991) On the formation of large subglacial lakes Canadian J Earth Sci **28** 1975-1981

Shoemaker, E M (1992a) Subglacial floods and the origin of low-relief ice-sheet lobes J Glaciol, **38**, 105-112

Shoemaker, E M (1992b) Water sheet outburst floods from the Laurentide Ice Sheet Can J Earth Sci , **29**, 1250-1264

Shreve, R L (1972) Movement of water in glaciers J Glaciol , **62**, 205-214

Shreve, R L (1985a) Esker characteristics in terms of glacier physics, Katahdin Esker System, Maine Geol Soc Am Bull , **96**, 639-646

Shreve, R L (1985b) Late Wisconsin ice-surface profile calculated from esker paths and types, Katadian Esker System, Maine Quat Res , **23**, 27-37

Siegert, M J (2000) Antarctic subglacial lakes Earth Sci Rev , **50**, 29-50

Siegert, M J and Ridley, J K (1998) Determining basal ice sheet conditions at Dome C, central East Antarctica, using satellite radar altimetry and airborne radio-echo sounding information J Glaciol , **44**, 1-8

Siegert, M J , Dowdeswell, J A , Gorman, M R and McIntyre, N F (1996) An inventory of Antarctic sub-glacial lakes Antarct Sci , **8**, 281-286

Sugden, D E , Denton, G H and Marchant, D R (1991) Subglacial meltwater channel systems and ice sheet overriding, Asgard Range, Antarctica Geogr Ann , **73A**, 109-121

Yokoyama, Y , Lambeck, K , Deckker, P D , Johnston, P and Fifield, L K (2000) Timing of the Last Glacial Maximum from observed sea-level minima Nature, **406**, 713-716

Yokoyama, Y , Lambeck, K , Deckker, P D , Johnston, P and Fifield, L K (2001) Collection Timing of the Last Glacial Maximum from observed sea-level minima Nature, **412**, 99

Yoshida, M , Yoshida, Y , Ando, H , Ishikawa, T and Tatsumi, T (1976) Geological map of Skallen Antarctic Geological Map Series, Sheet 9 Tokyo, National Institute of Polar Research

Yoshida, Y (1983) Physiography of the Prince Olav and the Prince Harald Coasts, East Antarctica Mem Natl Inst Polar Res , Series C (Earth Sci), **13**, 1-76

Watanabe, O , Fujii, Y , Nishio, F and Motoyama, H (1992) Position, elevation, ice thickness and bedrock elevation of stations along the routes in East Queen Maud Land and Enderby Land, East Antarctica JARE Data Rep , **180** (Glaciology 19), 143 p

(Received January 28, 2002, Revised manuscript accepted May 21, 2002)